Materials Today Bio 4 (2019) 100034

Contents lists available at ScienceDirect

Materials Today Bio

journal homepage: www.journals.elsevier.com/materials-today-bio

Introduction of lactobionic acid ligand into mixed-charge nanoparticles to realize in situ triggered active targeting to hepatoma cells

H. Li [a], X. Li [a], Y. Wang, J. Ji [*]

MOE Key Laboratory of Macromolecular Synthesis and Functionalization, Department of Polymer Science and Engineering, Zhejiang University, Hangzhou 310027, China

ARTICLE INFO

Keywords:
Mixed-charge
Antifouling
Active targeting
pH sensitivity

ABSTRACT

To overcome the dilemma between passive tissue targeting and active cell targeting, nanomaterials are often required to exhibit the transition from 'stealth' to 'active targetable' in response to the pathological microenvironment. Here, we introduced a ternary surface modification method that incorporating active targeting ligand lactobionic acid with pH-sensitive mixed-charge surface. The resulted mixed-charge gold nanoparticles (LA@MC-GNPs) showed resistance to non-specific adsorption of proteins and uptake by HepG2 cells at normal tissue pH 7.4, while they underwent pH-sensitive aggregation and recovered active targeting capability at tumor acidic pH 6.5. The ternary surface modification method provided a simplest strategy to solve the dilemma between passive and active targeting of nanomedicine.

1. Introduction

Targeting to specific tissues and cells has emerged as a major challenge for nanomedicine to achieve desired therapeutic outcomes with minimized side effects [1,2]. For nanomedicine aimed at cancer treatment, passive tissue targeting is often realized via the enhanced permeability and retention (EPR) effect, as the leaky vascular and inefficient lymphatic drainage in tumor allow extravasation and retention of nanoparticles at tumor site [3,4]. Designing nanoparticles with targeting ability to physiological characteristics of tumor microenvironment was proved to further promote the accumulation of nanoparticles at tumor tissue; hence, improved passive tissue targeting could be achieved [5,6]. For example, we previously reported a pH-sensitive mixed-charge gold nanoparticle (MC-GNP) that could target to tumor acidic microenvironment [6]. At the pH of blood and normal tissues, the MC-GNPs remained stable and 'stealth' because of the zwitterionic nature, which endowed nanoparticles with long circulation time to reach tumor tissues efficiently. After leak into tumor tissue through EPR effect, the MC-GNPs formed large aggregates in response to acidic milieu, which hindered backflow of nanoparticles to bloodstreams and promoted uptake by cancer cells. Hence, the MC-GNPs exhibited much higher tumor accumulation and retention than non-sensitive polyethylene glycol (PEG)–modified GNPs.

Active targeting, on the other hand, could endow nanoparticles with specific cell interaction and enhanced uptake through ligand-receptor recognition [1,7–9]. However, active targeting ligands attached on the surface of nanoparticles could be easily recognized by immune system, which accelerates clearance of nanoparticles by the host and lowers their chance to reach target site [10–13]. Sometimes, the presence of active targeting moiety even brings no benefit for nanoparticles to accumulate at lesion site as the blood circulation time is greatly shortened [12]. Modifying nanoparticles with antifouling materials such as PEG could partially relieve this problem via inhibiting non-specific interaction [14–16], but the antifouling surface of nanoparticles would meanwhile hamper the recognition and interaction between nanoparticles and target cells [17]. To this end, great efforts have been made to develop nanoparticles' surface with pathological environment sensitivity to realize the change from 'stealth' to 'active targetable' at lesion site [18]. For instance, Kuai et al. [19] comodified liposomes with thiolytic cleavable PEG- and cell-penetrating peptide TAT (AYGRKKRRQRRR). Before arriving at tumor tissue, the PEGylated surface benefited the blood circulation time so that the liposomes could passively accumulate at tumor site. Upon entering tumor tissue, the PEG chain on the liposomes' surface would be removed by a cleaving reagent L-cysteine to expose the active peptide TAT, which promoted cell uptake of the liposomes. Similarly, Hashiba et al. [20] modified lipid nanoparticle with pH-labile PEG coatings to realize both long time circulation at blood pH and in situ triggered active targeting ability at tumor acidic milieu. The aforementioned shield/deshield strategies have shown effectiveness in solving the

* Corresponding author.
E-mail address: jijian@zju.edu.cn (J. Ji).
[a] These authors contributed equally.

https://doi.org/10.1016/j.mtbio.2019.100034
Received 22 August 2019; Received in revised form 17 October 2019; Accepted 21 October 2019
Available online 25 October 2019

dilemma between passive and active targeting; however, the related materials were often too complex to prepare, which hindered their practical application.

As aforementioned, the MC-GNPs showed 'stealth' property with long blood circulation time at normal tissue pH, whereas they formed aggregates and promoted passive accumulation in tumor tissues at tumor acidic pH [6]. The transition of the MC-GNPs between different pH was merely resulted from the variation of surface charge, as the protonation state of carboxyl groups in surface ligands changed along pH. Compared with the nanoplatforms involved with cleavage of antifouling coatings, the MC-GNPs were much simpler in structure to realize transition from stealth to non-stealth in response to environmental stimuli. However, it is still unknown if the mixed-charge surface modification could work in harmony with active targeting ligands. In this work, we use thiolated lactobionic acid (HS-LA) with hepatoma cell targeting ability as a model active targeting ligand to comodify GNPs' surface with mixed-charge ligands (HS–$(CH_2)_{10}$–COOH and HS–$(CH_2)_{10}$–$N(CH_3)_3$Br). It is hypothesized that the obtained LA@MC-GNPs remains 'stealth' to resist non-specific adsorption of proteins and cell uptake at pH 7.4 because of the mixed-charge nature, whereas forms aggregates and exerts ligand-receptor recognition at pH 6.5 to enhance cancer cellular uptake (Fig. 1). It may provide a simplest approach to overcome the dilemma between passive targeting and active targeting.

2. Materials and methods

2.1. Materials

11-Mercaptoundecanoic acid (HS–$(CH_2)_{10}$–COOH, MUA) was purchased from J&K Chemical Ltd. (Shanghai, China). (10-Mercaptodecyl) trimethylammonium bromide (HS–$(CH_2)_{10}$–$N(CH_3)$, TMA) was prepared in accordance with the literature reported previously [21]. (2,3,5,6-tetrahydroxy-4-((3,4,5-trihydroxy-6-(hydroxymethyl)tetrahydro-2H-pyran-2-yl) oxy)hexanoyl)cysteine (HS-LA) was prepared by the N–hydroxysuccinimide (NHS)/N-(3-dimethylaminopropyl)- N′-ethylcarbodiimide (EDC) reaction between lactobionic acid (LA) and cysteine in accordance with the study by Chen [22]. Bovine serum albumin (BSA) was bought from Life Science Products & Services. Human hepatoma cell line (HepG2) was purchased from China Center for Typical Culture Collection. pH 7.4 and pH 6.5 Roswell Park Memorial Institute (RPMI) 1640 cell culture media was purchased from Genom (Hangzhou, China). 3-(4,5-dimethyl-2-thiazolyl)-2, 5-diphenyl-2-H-tetrazolium bromide (MTT) was obtained from YEASEN Biotechnology (Shanghai, China). Hydrogen tetrachloroaurate hydrate ($HAuCl_4{\cdot}4H_2O$), trisodium citrate dehydrate ($C_6H_5Na_3O_7{\cdot}2H_2O$) and all other reagents were purchased from Sinopharm Chemical Reagent Co., Ltd. (Shanghai, China).

2.2. Preparation of GNPs

The 15-nm GNPs were prepared by standard citrate reduction method reported previously [23]. Briefly, 5 mL of 10 mM $HAuCl_4{\cdot}4H_2O$ solution was added to 45 mL of Milli-Q water with vigorous stirring and heated to 160 °C. Then, 5.8 mL of 38.8 mM freshly prepared sodium citrate was added to the boiling solution. After the solution color turned from bright yellow to wine red, the solution was kept heating for another 15 min, and then cooled to room temperature.

2.3. Preparation of MC-GNPs and LA@MC-GNPs

The premixed ligand solution was used to modify GNPs. For MC-GNPs, the ligand solution was prepared by mixing 10 mM MUA and TMA with a molar ratio of 1:1. For LA@MC-GNPs, the ligand solution was prepared by mixing 10 mM MUA, TMA, and HS-LA. The molar ratio among the three ligands is 0.4:0.4:0.2. The 1 mL ligand solution was added to 10 mL of the freshly prepared GNPs solution. Immediately, 1 M NaOH was used to adjust the solution pH to 7–8. The solution was kept stirring at room temperature for another 24 h. Then the solution was purified through centrifugation 3 times under the condition of 15,000 rpm/15 min. To maintain the stability of the final concentrated nanoparticle solution, 10 mM phosphate buffer (PB) with pH 9.0 was used to adjust the solution pH.

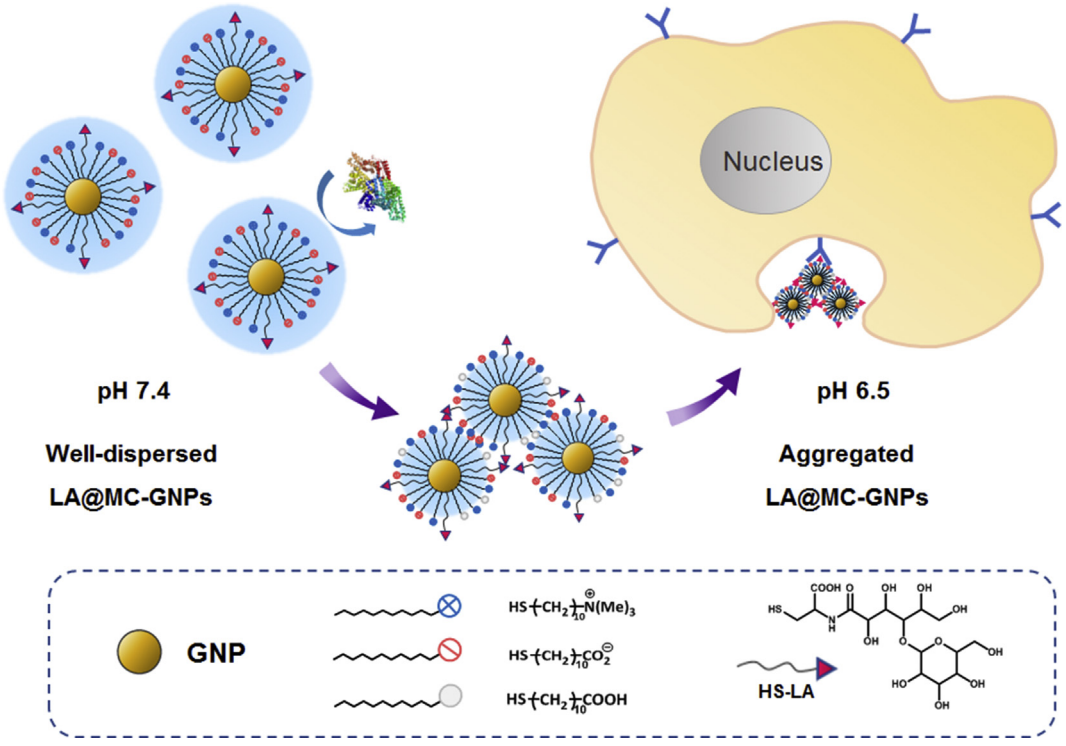

Fig. 1. Schematic illustration of the pH sensitive behaviors of the LA@MC-GNPs. The LA@MC-GNPs are stealth at pH 7.4 while they exhibit active cell targeting at pH 6.5.

2.4. Fourier-transform infrared spectroscopy

The nanoparticles solution was centrifugated at 15,000 rpm for 15 min to remove most of the water and subjected to vacuum drying to get rid of residual water. Then samples were prepared through KBr pellet method and subjected to collect Fourier-transform infrared (FT-IR) spectra (Bruker Vector2).

2.5. pH sensitivity

The pH sensitivity of MC-GNPs and LA@MC-GNPs was studied by incubating the nanoparticles in 10 mM PB and RPMI 1640 cell culture media of different pH. The colloidal stability of nanoparticles in different pH environment was studied using the ultraviolet-visible spectra (UV-Vis, UV-2505, Shimadzu). The morphology and colloidal stability were analyzed by transmission electron microscope (TEM, HT-7700, Hitachi). The hydrodynamic size of nanoparticles was determined by dynamic light scattering (, Zetasizer Nano ZS, Malvern).

2.6. Protein adsorption assay

Non-specific protein adsorption of MC-GNPs and LA@MC-GNPs was studied by gel electrophoresis and hydrodynamic size change of GNPs in protein-containing solution. For gel electrophoresis, the GNPs were premixed in phosphate buffer saline (PBS) and 10 mg mL^{-1} BSA solution, respectively with volume ratio being 1:1. Then, 10 μL of premixed GNP solution was loaded on agarose gel (1%, w/w) buffered with 0.5 × Tris-Boric acid-EDTA (TBE) buffer. Gel electrophoresis was conducted in 0.5 × TBE buffer at 120 V for 15 min and recorded by a digital camera. For hydrodynamic size change of GNPs in protein-containing solution, the nanoparticles size of LA@MC-GNPs in pH 7.4 RPMI 1640 with 10% fetal bovine serum (FBS) within 24 h was collected.

2.7. Cell uptake

HepG2 cells were seeded in a 24-well plate with a density of 100,000/well and cultured at 37 °C with 5% CO_2 for 24 h. Then, the pH 7.4 RPMI 1640 cell culture media was replaced by MC-GNPs and LA@MC-GNPs samples that premixed with pH 7.4 and pH 6.5 RPMI 1640 cell culture media (fetal bovine serum (FBS) free). The concentration of GNP was 0.3 nM. After 6 h of incubation, the HepG2 cells were washed with PBS 3 times and subsequently added with 200 μL freshly prepared aqua regia. Then 800 μL of Milli-Q water was added to each well to terminate the interaction with aqua regia. Twenty-fold diluted samples were subjected to inductively coupled plasma mass spectrometry (, XSeries II, Thermo Scientific) to detect the content of gold element. To block asialoglycoprotein receptor, HepG2 cells were pretreated with 10 mg mL^{-1} of LA for 2 h. Statistical significance was tested by analysis of variance.

2.8. Cytotoxicity

HepG2 cells were seeded in a 96-well plate with a density of 5,000/well and cultured for 24 h. Then, MC-GNPs and LA@MC-GNPs samples that premixed with pH 7.4 and pH 6.5,respectively, RPMI 1640 cell culture media (FBS free) were used to incubate HepG2 cells for another 24 h. After 24 h incubation, the HepG2 cells were washed with PBS 3 times and subjected to standard MTT assay.

3. Results and discussion

3.1. pH sensitivity of LA@MC-GNPs

The LA@MC-GNPs were prepared in a similar way as MC-GNPs by modifying 15 nm GNPs' surfaces using a mixture of 11-mercaptoundecanoic acid (MUA), (10-mercaptodecyl) trimethylammonium bromide (TMA) and HS-LA. The feed ratio among three ligands was chosen to be 0.4:0.4:0.2, as futher increasement of the LA content to 40% or 60% could lead to undesired instability of LA@MC-GNPs in physiological pH 7.4 (Fig. S1). Compared to MC-GNPs, a bending vibration absorption peak of N–H bond was observable in the FT-IR spectrum of LA@MC-GNPs (Fig. S2). As HS-LA ligand could be the only source for N–H bond, it meant that the GNP's surface was successfully modified with HS-LA ligands for LA@MC-GNPs.

Then, the pH sensitivity of the MC-GNPs and LA@MC-GNPs was carefully studied. For GNPs, solution color would turn blue or purple from wine red when aggregation happened and there would be a redshift of absorption peak in UV-Vis spectrum. Hence colloidal stability of GNPs could be determined from solution color and location of absorption peak in UV-Vis spectra. From Fig. 2A and B, it could be found out that MC-GNPs aggregated from pH 6.8 to pH 4 and dispersed at all other tested pH. This was similar with the pH sensitive behaviors of MC-GNPs reported before [6]. At high pH, the surface charge of MC-GNPs was overall negative because of the presence of deprotonated carboxyl group. Hence, the MC-GNPs could be stabilized by electrostatic repulsion and hydration effect. When the solution pH went down, the carboxyl group on the nanoparticles' surface would be gradually protonated, which resulted in a loss of carboxylic negative charge and increasement of hydrogen bonding between carboxyl groups from different nanoparticles. In addition, the variation in surface charge composition would weaken the hydration layer of MC-GNPs at the same time. When the overall repulsive interaction surpassed the overall attractive interaction, the MC-GNPs would aggregate. At certain low pH, the MC-GNPs were overall positively charged because the positive charge originated from the quaternary ammonium groups surpassed the negative charge of the remained deprotonated carboxylic groups, which led to dispersion of MC-GNPs through electrostatic repulsion and hydration effect. From Fig. 2A and C, it could be found out that LA@MC-GNPs showed the same pH sensitivity as MC-GNPs. That is, the LA@MC-GNPs also aggregated from pH 6.8 to pH 4.0 and remained dispersed at all other tested pH. Thus, the presence of hydrophilic LA ligands had no significant impact on the pH sensitive behaviors of GNPs.

MC-GNPs were proved to have similar pH sensitivity in protein-containing environment such as cell culture media [6]. To evaluate the pH sensitivity in complex environment such as cell culture media, the LA@MC-GNPs were incubated in pH 7.4 and pH 6.5 RPMI 1640 cell culture media, respectively. Fig. 3A showed that the LA@MC-GNPs dispersed in pH 7.4 cell culture media and aggregated at pH 6.5 cell culture media. From the results of the hydrodynamic size distribution in Fig. 3B, it could be seen that the size of LA@MC-GNPs changed from a single nanoparticle size to around 200 nm, which indicated occurrence of aggregation from pH 7.4 to pH 6.5. The TEM images suggested the LA@MC-GNPs dispersed well at pH 7.4 RPMI 1640 cell culture media (Fig. 3C and Fig. S3A), whereas they formed aggregates at pH 6.5 RPMI 1640 cell culture media (Fig. 3D and Fig. S3B). These results showed that the sensitivity to tumor acidic pH of the LA@MC-GNPs remained in complex media.

3.2. Resistance to non-specific protein adsorption of LA@MC-GNPs

The MC-GNPs showed resistance to non-specific protein adsorption, namely antifouling ability because of the zwitterionic nature of the nanoparticles' surface [6]. It is an important question that if the GNPs still possessed the antifouling property after introducing the LA ligand into nanoparticles' surface. The LA@MC-GNPs had a zeta potential of −9.78 ± 0.09 mV, which was comparable with the zeta potential of the previously reported zwitterionic MC-GNPs [24]. Similar to MC-GNPs, the mobility of LA@MC-GNPs in gel electrophoresis was not influenced by the preincubation with BSA (Fig. 4A), suggesting that the LA@MC-GNPs could resist to non-specific adsorption of BSA. That is, introducing LA ligand into the mixed-charge surface modification did not impact nanoparticles to acquire stealth characteristic. The LA@MC-GNPs were further incubated at pH 7.4 RPMI 1640 with 10% FBS to study the change

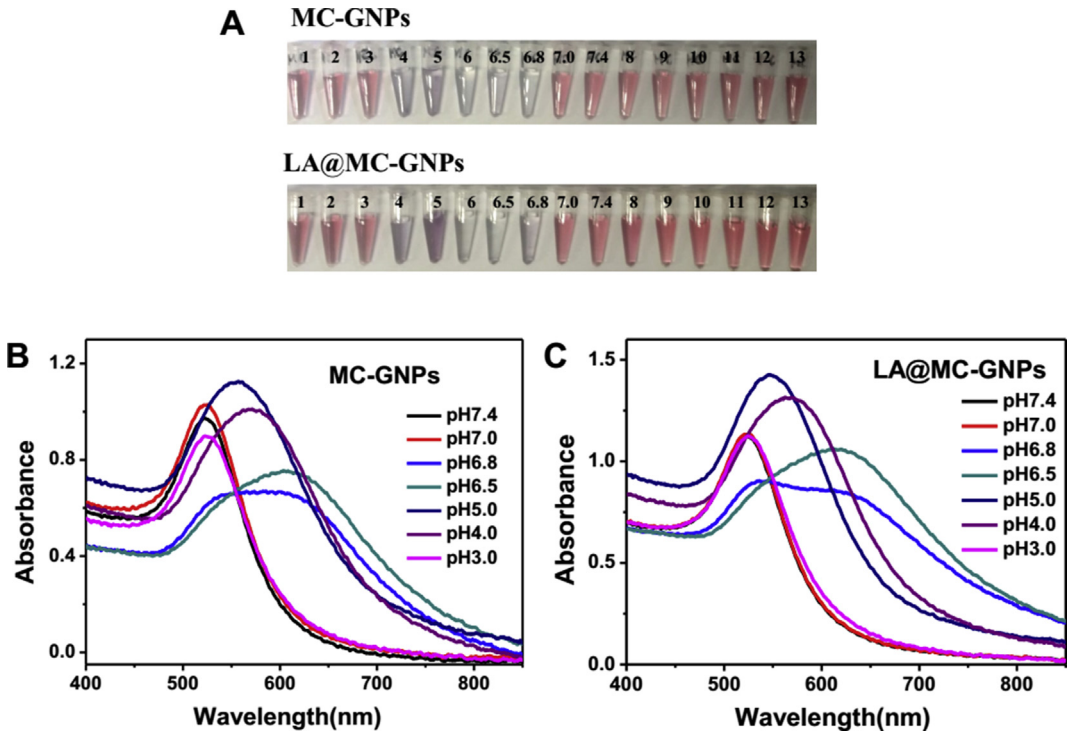

Fig. 2. (A) Digital images of MC-GNPs and LA@MC-GNPs in PB of different pH. UV-Vis spectra of (B) MC-GNPs and (C) LA@MC-GNPs in PB of different pH. PB, phosphate buffer.

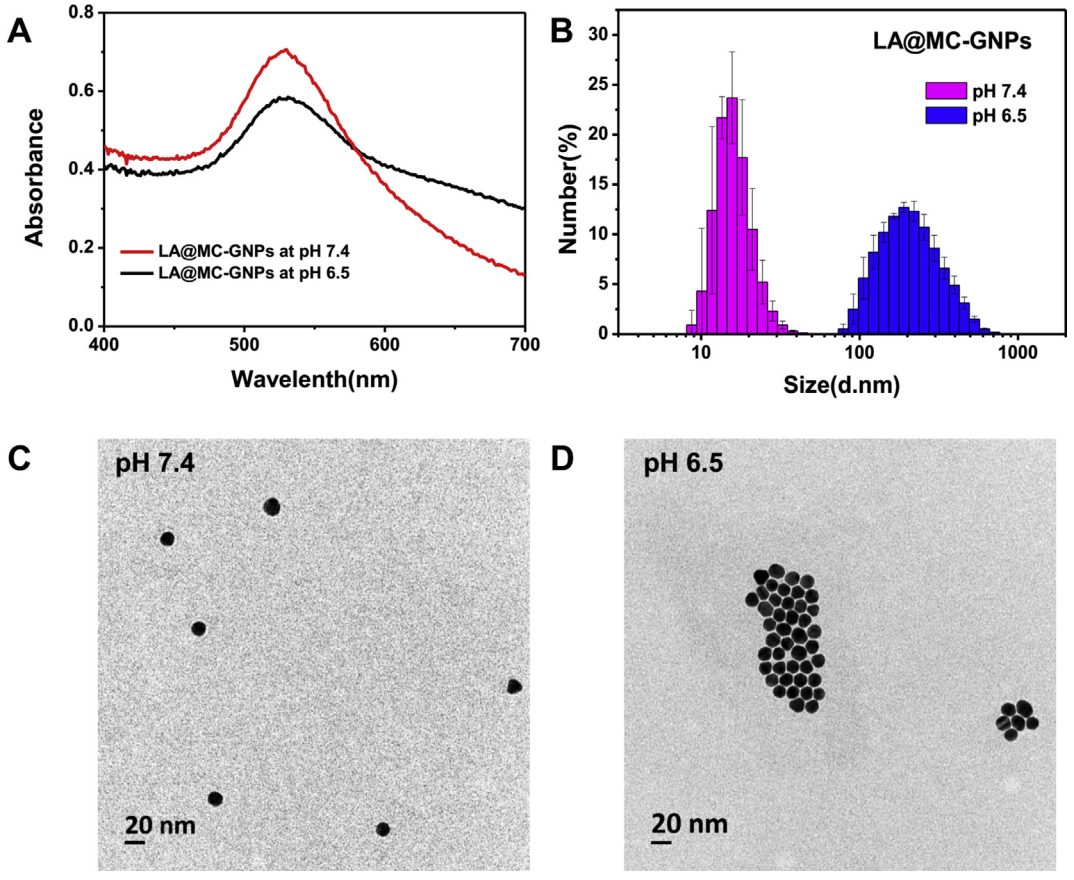

Fig. 3. (A) UV-Vis spectra and (B) hydrodynamic size distribution of LA@MC-GNPs in pH 7.4 and pH 6.5 RPMI 1640 cell culture media. TEM images of LA@MC-GNPs in (C) pH 7.4 and (D) pH 6.5 RPMI 1640 cell culture media.

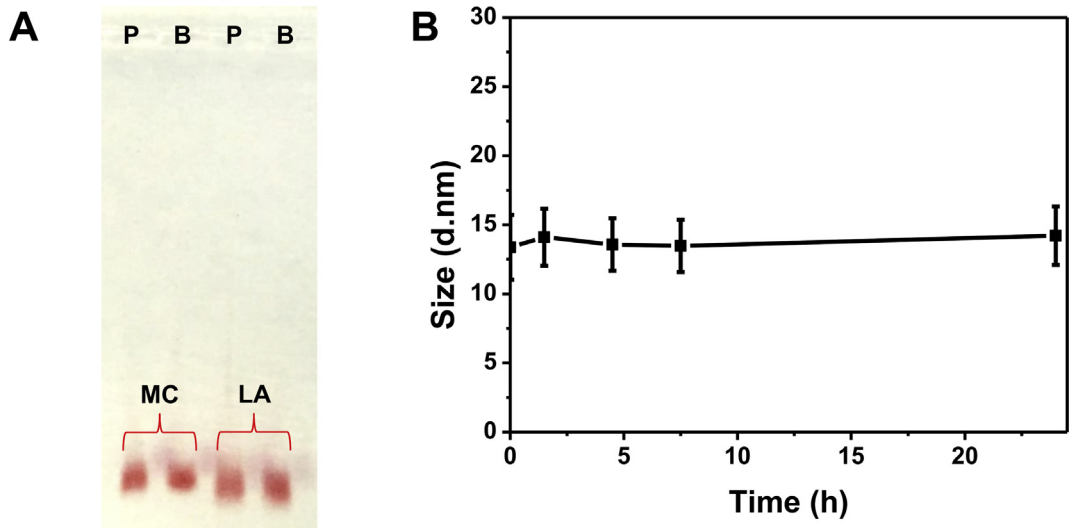

Fig. 4. (A) Gel images of BSA adsorption assay for MC-GNPs and LA@MC-GNPs (P represented PBS, B represented BSA). (B) Hydrodynamic size distribution within 24 h of LA@MC-GNPs incubating at pH 7.4 RPMI 1640 containing 10% FBS. BSA, bovine serum albumin; PBS, phosphate buffered saline.

of hydrodynamic size of GNPs along time. It could be seen from Fig. 4B, the hydrodynamic size of LA@MC-GNPs did not show obvious change within 24 h, indicating that the LA@MC-GNPs neither adsorbed proteins in solution nor formed aggregates to result in an increasement in hydrodynamic size. This further proved the ability of LA@MC-GNPs to resist non-specific protein adsorption. The antifouling ability of LA@MC-GNPs was deduced to originate from the hydration layer formed on the zwitterionic mixed-charge surface.

3.3. Cell uptake of LA@MC-GNPs by HepG2 cells

As LA had specific targeting ability to hepatoma cells [22], HepG2 cell was used as model hepatoma cell to study the cell uptake of MC-GNPs and LA@MC-GNPs at pH 7.4 and pH 6.5,respectively. From Fig. 5, it could be seen that the MC-GNPs and LA@MC-GNPs both showed low cell uptake by HepG2 cells at pH 7.4. As it was proved that the antifouling surface of nanoparticles may hinder their interaction with biological units such as cells [15,25], the low cell uptake at pH 7.4 was believed to be the consequence of the antifouling ability of MC-GNPs and LA@MC-GNPs. At pH 6.5, the MC-GNPs showed increased cell uptake than at pH 7.4. This was in accordance with the pH-sensitive uptake of MC-GNPs reported before [6]. Compared with pH 7.4, the amount of protonated carboxyl groups on MC-GNPs' surfaces increased at pH 6.5, which led to the loss of part of negative charges and enhanced local positive charge. As positive surface charge of nanoparticles was proved to be more ready for cell uptake [26], the increased positive charge on the MC-GNPs' surface would contribute to the enhanced cell uptake. The aggregation of MC-GNPs at pH 6.5 would also promote cell uptake through the sedimentation-driven uptake [27]. For LA@MC-GNPs, the cell uptake at pH 6.5 was also significantly enhanced than that at pH 7.4, which should be related to the loss of carboxylic negative charge and aggregation of the GNPs. More interestingly, the cell uptake of LA@MC-GNPs was much higher than that of MC-GNPs at pH 6.5. It has been proved that the specific interaction between targeting ligands on nanoparticles' surface and receptors on cell surface could promote the selective uptake of nanoparticles [28,29]. Hence, the enhanced cell uptake than MC-GNPs should be the result of specific recognition of LA ligands on LA@MC-GNPs by asialoglycoprotein receptors on HepG2 cells. To evaluate the contribution of LA ligands to cell uptake, the asialoglycoprotein receptors on HepG2 cells were blocked in advance. From Fig. 5, it could be found out that at pH 6.5, there was no obvious change in cell uptake of MC-GNPs with block pretreatment. In contrast, the cell uptake of LA@MC-GNPs was significantly inhibited after block pretreatment. Herein, the uptake of LA@MC-GNPs by HepG2 cells were asialoglycoprotein receptor–dependent. The enhanced cell uptake of LA@MC-GNPs than MC-GNPs at tumor acidic pH 6.5 was originated from the specific interaction between LA and the receptors on HepG2 cells. The result of molecular dynamic simulation conducted by Liu and Zhou [30] showed that the mixed-charge surface had strong hydration effect that could resist non-specific adsorption of proteins through hydration layer. When the composition of surface charge changed to the extent that deviated from zwitterionic state, the hydration effect would greatly weaken and the surface would turn to a fouling state. In this sense, the active interaction between targeting ligand LA and HepG2 cells might be related to the variation in hydration layer along with the pH change. It is hypothesized that the LA@MC-GNPs could resist non-specific interaction with proteins and cells through hydration layer at pH 7.4, whereas form aggregates with local positive charge and expose active targeting ligand LA to promote specific cell uptake at pH 6.5 because of the weakened hydration layer (Fig. 1).

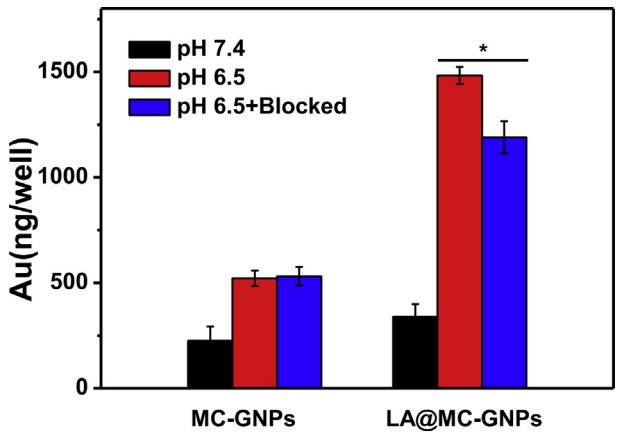

Fig. 5. Cell uptake of the MC-GNPs and LA@MC-GNPs by HepG2 cells and those with blocked asialoglycoprotein receptors ($n = 3$). Asterisk indicates significant difference, $^*p<0.05$.

3.4. Cytotoxicity of LA@MC-GNPs

The toxicity of MC-GNPs and LA@MC-GNPs to HepG2 cells at pH 7.4 and pH 6.5 was evaluated in vitro. From the results of MTT assay in

Fig. S4, it could be found out that MC-GNPs and LA@MC-GNPs did not show noticeable cytotoxicity at concentration of 0.025 nM, 0.05 nM, 0.2 nM, 0.3 nM, and 0.4 nM. This indicated that the surface modification by mixed-charge ligands and active targetable LA would not introduce cytotoxicity to GNPs.

4. Conclusions

In summary, we developed a novel nanoplatform LA@MC-GNPs whose surface was integrated with mixed-charge components and active targeting ligand LA. The LA@MC-GNPs showed zwitterionic nature at pH 7.4 that could resist non-specific interaction with proteins and cancer cells, whereas formed aggregates and recalled the active targeting ability at pH 6.5. Thus, the combination of pH sensitivity of mixed-charge moiety and bioactivity of active targeting ligand LA was proved to be capable of site-specific activation of biofunction, which provided a simplest way to overcome the dilemma between passive tissue targeting and active cell targeting.

Declaration of Competing Interest

The authors declare that they have no known competing financial interests or personal relationships that could have appeared to influence the work reported in this paper.

Acknowledgments

Financial support from the Science and Technology Program of Zhejiang Province (2016C04002), Fundamental Research Funds for the Central Universities (2017XZZX001-03B) and National Natural Science Foundation of China (21574114) is gratefully acknowledged.

Appendix A. Supplementary data

Supplementary data to this article can be found online at https://doi.org/10.1016/j.mtbio.2019.100034.

References

[1] D. Fabienne, F. Olivier, P. Véronique, To exploit the tumor microenvironment: passive and active tumor targeting of nanocarriers for anti-cancer drug delivery, J. Control. Release 148 (2010) 135–146, https://doi.org/10.1016/j.jconrel.2010.08.027.
[2] N. Bertrand, J. Wu, X. Xu, N. Kamaly, O.C. Farokhzad, Cancer nanotechnology: the impact of passive and active targeting in the era of modern cancer biology, Adv. Drug Delivery Rev. 66 (2014) 2–25, https://doi.org/10.1016/j.addr.2013.11.009.
[3] K. Greish, Enhanced permeability and retention (EPR) effect for anticancer nanomedicine drug targeting, Methods Mol. Biol. 624 (2010) 25–37, https://doi.org/10.1007/978-1-60761-609-2_3.
[4] H. Maeda, G.Y. Bharate, J. Daruwalla, Polymeric drugs for efficient tumor-targeted drug delivery based on EPR-effect, Eur. J. Pharm. Biopharm. 71 (2009) 409–419, https://doi.org/10.1016/j.ejpb.2008.11.010.
[5] E.S. Lee, Z. Gao, Y.H. Bae, Recent progress in tumor pH targeting nanotechnology, J. Control. Release 132 (2008) 164–170, https://doi.org/10.1016/j.jconrel.2008.05.003.
[6] X. Liu, Y. Chen, H. Li, N. Huang, Q. Jin, K. Ren, J. Ji, Enhanced retention and cellular uptake of nanoparticles in tumors by controlling their aggregation behavior, ACS Nano 7 (2013) 6244–6257, https://doi.org/10.1021/nn402201w.
[7] N. Bertrand, J. Wu, X. Xu, N. Kamaly, O.C. Farokhzad, Cancer nanotechnology: the impact of passive and active targeting in the era of modern cancer biology, Adv. Drug Deliv. Rev. 66 (2014) 2–25, https://doi.org/10.1016/j.addr.2013.11.009.
[8] M. Sylvain, Targeting active cancer cells with smart bullets, Ther. Deliv. 8 (2017) 301–312, https://doi.org/10.4155/tde-2016-0088.
[9] J.D. Byrne, T. Betancourt, L.B. Peppas, Active targeting schemes for nanoparticle systems in cancer therapeutics, Adv. Drug Deliv. Rev. 60 (2008) 1615–1626, https://doi.org/10.1016/j.addr.2008.08.005.
[10] W.W.K. Cheng, T.M. Allen, Targeted delivery of anti-CD19 liposomal doxorubicin in B-cell lymphoma: a comparison of whole monoclonal antibody, Fab′ fragments and single chain Fv, J. Control. Release 126 (2008) 50–58, https://doi.org/10.1016/j.jconrel.2007.11.005.
[11] A. Gabizon, A.T. Horowitz, D. Goren, D. Tzemach, H. Shmeeda, S. Zalipsky, In vivo fate of folate-targeted polyethylene-glycol liposomes in tumor-bearing mice, Clin. Cancer Res. 9 (2003) 6551–6559, https://doi.org/10.1002/cncr.11858.
[12] K.M. McNeeley, A. Annapragada, R.V. Bellamkonda, Decreased circulation time offsets increased efficacy of PEGylated nanocarriers targeting folate receptors of glioma, Nanotechnology 18 (2007), https://doi.org/10.1088/0957-4484/18/38/385101, 385101.
[13] Z. Cheng, A.A. Zaki, J.Z. Hui, V.R. Muzykantov, A. Tsourkas, Multifunctional nanoparticles: cost versus benefit of adding targeting and imaging capabilities, Science 338 (2012) 903–910, https://doi.org/10.1126/science.1226338.
[14] J.V. Jokerst, T. Lobovkina, R.N. Zare, S.S. Gambhir, Nanoparticle PEGylation for imaging and therapy, Nanomedicine 6 (2011) 715–728, https://doi.org/10.2217/nnm.11.19.
[15] S. Jiang, Z. Cao, Ultralow-fouling, functionalizable, and hydrolyzable zwitterionic materials and their derivatives for biological applications, Adv. Mater. 22 (2010) 920–932, https://doi.org/10.1002/adma.200901407.
[16] X. Liu, H. Li, Q. Jin, J. Ji, Surface tailoring of nanoparticles via mixed-charge monolayers and their biomedical applications, Small 10 (2015) 4230–4242, https://doi.org/10.1002/smll.201401440.
[17] S. Mishra, P. Webster, M.E. Davis, PEGylation significantly affects cellular uptake and intracellular trafficking of non-viral gene delivery particles, Eur. J. Cell Biol. 83 (2004) 97–111, https://doi.org/10.1078/0171-9335-00363.
[18] S. Hama, S. Itakura, M. Nakai, K. Nakayama, S. Morimoto, S. Suzuki, K. Kogure, Overcoming the polyethylene glycol dilemma via pathological environment-sensitive change of the surface property of nanoparticles for cellular entry, J. Control. Release 206 (2015) 67–74, https://doi.org/10.1016/j.jconrel.2015.03.011.
[19] R. Kuai, W. Yuan, Y. Qin, H. Chen, J. Tang, M. Yuan, Z. Zhang, Q. He, Efficient delivery of payload into tumor cells in a controlled manner by TAT and thiolytic cleavable PEG co-modified liposomes, Mol. Pharm. 7 (2010) 1816–1826, https://doi.org/10.1021/mp100171c.
[20] K. Hashiba, Y. Sato, H. Harashima, pH-labile PEGylation of siRNA-loaded lipid nanoparticle improves active targeting and gene silencing activity in hepatocytes, J. Control. Release 262 (2017) 239–246, https://doi.org/10.1016/j.jconrel.2017.07.046.
[21] H. Li, X. Liu, N. Huang, K. Ren, Q. Jin, J. Ji, "Mixed-charge self-assembled monolayers" as a facile method to design pH-induced aggregation of large gold nanoparticles for near-infrared photothermal cancer therapy, ACS Appl. Mater. Interfaces 6 (2014) 18930–18937, https://doi.org/10.1021/am504813f.
[22] W. Chen, Y. Zou, F. Meng, R. Cheng, C. Deng, J. Feijen, Z. Zhong, Glyco-nanoparticles with sheddable saccharide shells: a unique and potent platform for hepatoma-targeting delivery of anticancer drugs, Biomacromolecules 15 (2014) 900–907, https://doi.org/10.1021/bm401749t.
[23] G. Frens, Controlled nucleation for the regulation of the particle size in monodisperse gold suspensions, Nat. Phys. Sci. 241 (1973) 20–22, https://doi.org/10.1038/physci241020a0.
[24] X. Liu, J. Qiao, J. Ying, J. Jian, Minimizing nonspecific phagocytic uptake of biocompatible gold nanoparticles with mixed charged zwitterionic surface modification, J. Mater. Chem. 22 (2012) 1916–1927, https://doi.org/10.1039/C1JM14178C.
[25] A.K. Nowinski, A.D. White, A.J. Keefe, S. Jiang, Biologically inspired stealth peptide-capped gold nanoparticles, Langmuir 30 (2014) 1864–1870, https://doi.org/10.1021/la404980g.
[26] G. Sahay, D.Y. Alakhova, A.V. Kabanov, Endocytosis of nanomedicines, J. Control. Release 145 (2010) 182–195, https://doi.org/10.1016/j.jconrel.2010.01.036.
[27] A. Alexandre, W.C.W. Chan, Effect of gold nanoparticle aggregation on cell uptake and toxicity, ACS Nano 5 (2011) 5478–5489, https://doi.org/10.1021/nn2007496.
[28] H. Gao, W. Shi, L.B. Freund, Mechanics of receptor-mediated endocytosis, Proc. Natl. Acad. Sci. U. S. A. 102 (2005) 9469–9474, https://doi.org/10.1073/pnas.0503879102.
[29] L. Zhang, W. Fischer, E. Pippel, G. Hause, M. Brandsch, M. Knez, Receptor-mediated cellular uptake of nanoparticles: a switchable delivery system, Small 7 (2011) 1538–1541, https://doi.org/10.1002/smll.201100238.
[30] J. Liu, J. Zhou, Hydrolysis-controlled protein adsorption and antifouling behaviors of mixed charged self-assembled monolayer: a molecular simulation study, Acta Biomater. 40 (2016) 23–30, https://doi.org/10.1016/j.actbio.2016.04.044.